Time-stretch microscopy based on time-wavelength sequence reconstruction from wideband incoherent source

Chi Zhang, Yiqing Xu, Xiaoming Wei, Kevin K. Tsia, and Kenneth K. Y. Wong

Citation: Applied Physics Letters **105**, 041113 (2014); doi: 10.1063/1.4890861
View online: http://dx.doi.org/10.1063/1.4890861
View Table of Contents: http://scitation.aip.org/content/aip/journal/apl/105/4?ver=pdfcov
Published by the AIP Publishing

Time-stretch microscopy based on time-wavelength sequence reconstruction from wideband incoherent source

Chi Zhang,[a] Yiqing Xu, Xiaoming Wei, Kevin K. Tsia, and Kenneth K. Y. Wong[b]
Photonic Systems Research Laboratory, Department of Electrical and Electronic Engineering, The University of Hong Kong, Pokfulam Road, Hong Kong

(Received 17 April 2014; accepted 10 July 2014; published online 29 July 2014)

Time-stretch microscopy has emerged as an ultrafast optical imaging concept offering the unprecedented combination of the imaging speed and sensitivity. However, dedicated wideband and coherence optical pulse source with high shot-to-shot stability has been mandated for time-wavelength mapping—the enabling process for ultrahigh speed wavelength-encoded image retrieval. From the practical point of view, exploiting methods to relax the stringent requirements (e.g., temporal stability and coherence) for the source of time-stretch microscopy is thus of great value. In this paper, we demonstrated time-stretch microscopy by reconstructing the time-wavelength mapping sequence from a wideband incoherent source. Utilizing the time-lens focusing mechanism mediated by a narrow-band pulse source, this approach allows generation of a wideband incoherent source, with the spectral efficiency enhanced by a factor of 18. As a proof-of-principle demonstration, time-stretch imaging with the scan rate as high as MHz and diffraction-limited resolution is achieved based on the wideband incoherent source. We note that the concept of time-wavelength sequence reconstruction from wideband incoherent source can also be generalized to any high-speed optical real-time measurements, where wavelength is acted as the information carrier. © *2014 AIP Publishing LLC*. [http://dx.doi.org/10.1063/1.4890861]

Time-stretch microscopy (e.g., serial time-encoded amplified microscopy (STEAM)[1] and its newer generation, asymmetric-detected time-stretch optical microscopy (ATOM)[2]) boasts an unprecedentedly high optical imaging speed without compromising the sensitivity and thus creates a paradigm shift in realizing high-throughput diagnostics in biomedicine[2–4] and ultrafast inspection in high-volume manufacturing.[5,6] A common core feature of time-stretch microscopy is its use of wideband sources, such as the femtosecond source and the supercontinuum (SC) source[7] for quasi-linear wavelength-to-time mapping, which is the central mechanism enabling ultrafast image acquisition. Considering the almost transform-limited wideband source, all the spectral components within the source bandwidth start at the same temporal point. Time-stretch through group velocity dispersion (GVD) is thus employed to realize the quasi-linear wavelength-to-time mapping,[1,8–10] as shown in Fig. 1(a). However, robust time-stretch operation imposes stringent requirements on the source, namely, the optical bandwidth, shot-to-shot stability, and coherence. Although stable SC source can be achieved with femtosecond pulses (e.g., the Ti:Sapphire mode-locked laser), such kind of ultra-short pulses require dedicated dispersion control and are often sensitive to perturbations.[11] Different schemes have been proposed and implemented to improve the picosecond pulse pumped SC source, such as feedback mechanism,[12] dispersion engineering,[13] and active seeding approaches.[14–17] However, all these mechanisms further increase the complexity of the SC source generation, and simpler wideband source is desirable.

Recently, we developed a parametric spectro-temporal analyzer (PASTA),[18] as a complementary modality of the ultrafast time-stretch spectroscopy,[19] and it has greatly enlarged the observation temporal window from short pulse to ~ns range.[20] By adding a time-lens in front of the dispersion, its output also reconstructs the wavelength information in the temporal domain. Comparing with conventional time-stretch microscopy in Fig. 1(a), which requires the linear wavelength-to-time mapping at the output, our PASTA coincidently performs similar feature in Fig. 1(b). Thus, PASTA is naturally compatible with the time-stretch microscopic system. The essential advantage of PASTA is its capability in observing arbitrary waveform within its observation window. As a result, the PASTA-based STEAM unprecedentedly relieves its source constraint beyond ultrashort-pulse

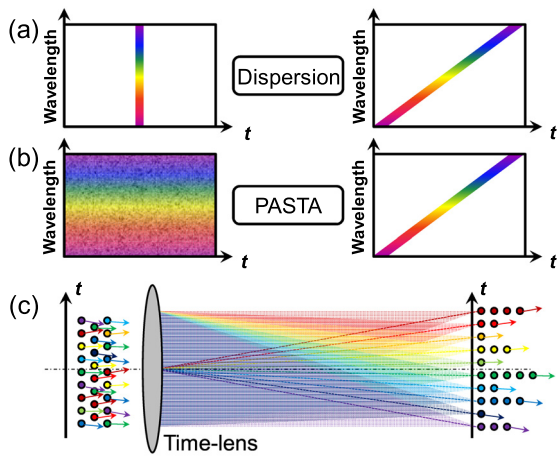

FIG. 1. Principle of reconstructing the time-wavelength sequence by PASTA system. (a) Time-stretching of the supercontinuum source in realizing the linear wavelength-to-time mapping; (b) the wideband incoherent source is reconstructed by PASTA system; (c) the mechanism of the PASTA system in reconstructing the temporal sequence of different colors.

[a]Electronic mail: chizheung@gmail.com
[b]Electronic mail: kywong@eee.hku.hk

source. Intriguingly, any wideband source (even the incoherent source) can realize the imaging functionality of STEAM, as illustrated in Fig. 1(b).

The PASTA system is based on the time-lens focusing mechanism, and it is implemented with swept pumped four-wave mixing (FWM).[21,22] Figure 1(c) illustrates how the PASTA system can reconstruct the time-wavelength sequence from wideband incoherent source. It is a temporal ray diagram, where the horizontal axis corresponds to the temporal dispersion, the vertical axis corresponds to the time, and the axial angle corresponds to the wavelength.[23] Each wavelength is labeled as a specified color, and at the input of the PASTA, the same color has the same axial angle. Therefore, identical color (wavelength) across the time-lens aperture will be rearranged after the output dispersion, as shown in Fig. 1(c). In addition to the time-wavelength sequence reconstruction, in the temporal domain, our PASTA system can also potentially amplify the optical power within the fiber medium, so as to enhance the imaging sensitivity.[8]

The experimental setup of the PASTA-based STEAM is shown in Fig. 2. The wideband incoherent source was provided from the amplified spontaneous emission (ASE) source of an erbium-doped fiber amplifier, and the wavelength range from 1536 nm to 1545 nm was filtered out to match the observation range of the PASTA system. Port 2 was the space-to-wavelength mapping stage: the wideband incoherent source was spatially dispersed by a diffraction grating, and focused at different positions (correspond to different wavelengths) of the samples. Here, the beam size after the fiber collimator was $W = 3$ mm, the group density of the grating is $D = 600$/mm, the angle of incidence is $\beta = 55°$, and the focal length of the lens is $f = 150$ mm. According to the diffraction principle, we can obtain the angle of diffraction $\theta = 6°$. Therefore, the wavelength resolution of this spectrally encoded system is

$$\delta\lambda = \frac{\lambda}{mN} = \frac{\lambda \cos\beta}{mWD}, \tag{1}$$

where m is the order of the diffraction (equals to 1 in our system) and N is the total number of slits illuminated. Here, we can obtain this wavelength resolution $\delta\lambda = 0.5$ nm. After the sample reflection, the spatial information was encoded onto the wavelength.

Port 3 was connected to the wavelength-to-time mapping stage, which was implemented by the single-lens PASTA.[18] Here, the time-lens was implemented with the parametric mixer,[21,22] as shown in the dashed box of Fig. 2. The swept-pump was stretched from a 7-ps pulse source (0.5-nm spectral width), and the focal and the output group-dispersion delay (GDD) were 2450 ps^2, which corresponded to the wavelength-to-time mapping relation of −0.508 nm/ns. Finally, the output signal was obtained by a single-pixel photodetector as well as a real-time oscilloscope (Agilent DSO-X 91604A, 16-GHz bandwidth). According to the discussion in Refs. 18 and 20, the 0.03-nm wavelength resolution in the PASTA system was smaller than that of the space-to-wavelength mapping, limited by the diffraction grating. Therefore, the whole system is a diffraction-limited system, and the overall resolution is 0.5 nm. To minimize the overlap of the neighboring periods, we have enlarged the temporal window of each frame to 20 ns, namely, increasing the wavelength range to 10 nm, which corresponds to the frame rate of 50 MHz. Therefore, there are 20 effective sampling points in a single frame. The detection sensitivity of the PASTA

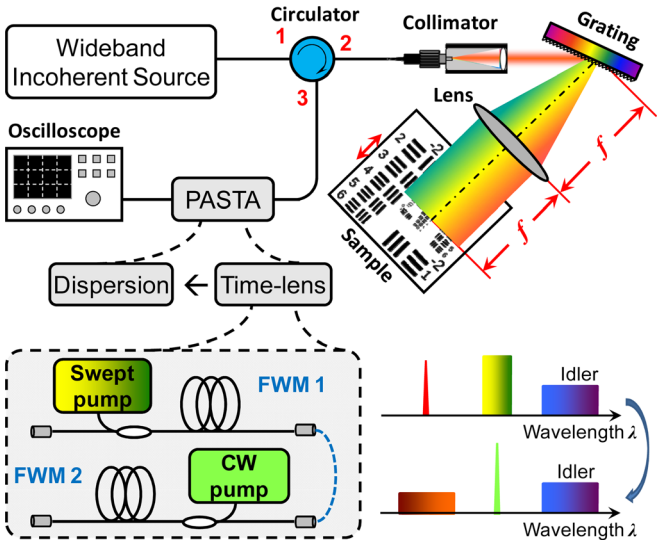

FIG. 2. Experimental setup of the PASTA based STEAM imaging system. The circulator directions described the sequence of the system: port 1 accepted the wideband ASE source, port 2 launched into the space-to-wavelength encoded part, and the reflected signal came to port 3 (PASTA). The bottom dashed box shows the detailed experimental schematic of the time-lens, as well as the PASTA system, and the wavelength conversions of the two-stage FWMs are shown in the right bottom figure.

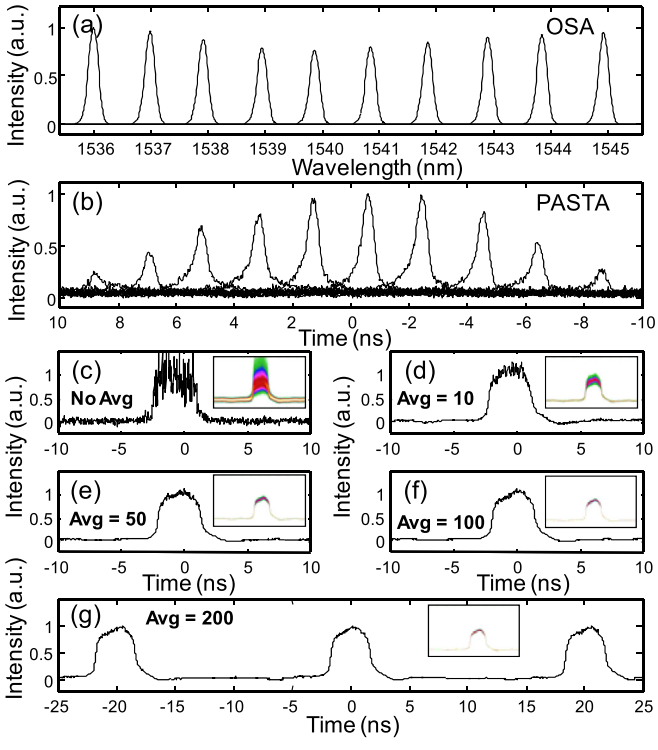

FIG. 3. Characteristics of the PASTA system in reconstructing the time-wavelength sequence of the wideband ASE source. (a) and (b) Tuning the 0.02-nm filter with 1-nm separation from 1536 nm to 1545 nm, and obtained the spectra from the conventional OSA and PASTA separately; (c)–(g) using PASTA to measure 2-nm ASE source, and changing the averaging time from no averaging, 10 times, 50 times, 100 times, to 200 times. The insets show the accumulated eye diagrams.

system is −32 dBm,[18] thus milliwatt level of illumination power on a lossy sample is able to be observed.

In order to verify the reconstructing ability of our PASTA system on wideband incoherent source, we first employed a variable bandwidth tunable band-pass filter (VBTBPF) to substitute the space-to-wavelength mapping by controlling the spectral width of the ASE source. The minimum passing wavelength bandwidth is 0.2 nm, which corresponds to 400-ps output pulsewidth in the PASTA system, and the results are shown in Fig. 3. We first used the minimum filter bandwidth (0.2 nm) to calibrate the wavelength positions by tuning the filter across the observation bandwidth with 1-nm separation. This result was compared with the measurement of a conventional optical spectrum analyzer (OSA, Yokogawa AQ6375), with 0.05-nm resolution as shown in Figs. 3(a) and 3(b). Their wavelength position matched very well, while the intensity envelope was decayed at the edge owing to the phase-mismatch of the FWM process in the PASTA system. Noted that the single-shot measurement of the ASE spectrum is quite noisy (Fig. 3(c)), and long-time averaging was required to provide the stable spectral shape (100 times in Fig. 3(f)). Here, we also show the effects of different number of averaging in Figs. 3(c)–3(g). The VBTBPF bandwidth was set as 2-nm, and centered at 1540 nm. We changed the number of averaging from zero, 10 times, 50 times, 100 times, to 200 times, and the insets show the accumulated eye diagrams. Figure 3(g) shows three frames averaged by 200 times, and each frame was separated by 20 ns (50-MHz frame rate).

It is observed from Fig. 3(b) that, by leveraging the 0.5-nm bandwidth pulse pump in the PASTA system, we resolved the spectral information of the 9-nm ASE source in the temporal domain. While in the dispersive stretching based STEAM system, a 9-nm imaging bandwidth usually requires a 9-nm pulse source. Therefore, our mechanism increases the spectral efficiency by a factor of 18. Back to the microscopy application, the VBTBPF was substituted by the space-to-wavelength mapping stages, and here the sample was placed on a translation stage, which was electrically controlled to construct the 2D images, shown as the red arrow in Fig. 2. According to the aforementioned discussion, the spectral resolution of our grating system is $\delta\lambda = 0.5$ nm,

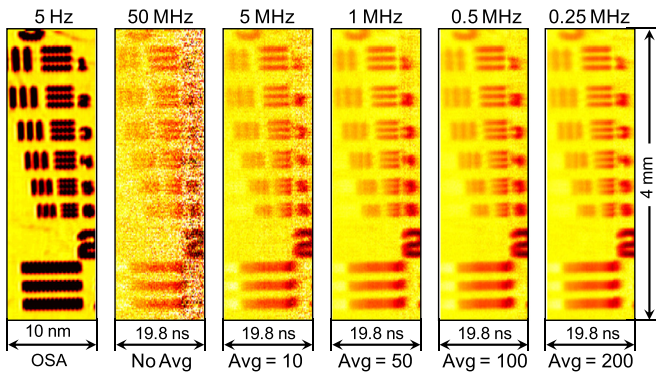

FIG. 4. Performances of the resolution target images (USAF 1951, Group 3). From left to right, OSA: encoded wavelength information captured by the conventional OSA; No Avg: captured by the PASTA system, without averaging; Avg = 10–200: captured by the PASTA system, and each frame was averaged by 10 times, 50 times, 100 times, and 200 times, respectively. Intensity variations among these STEAM figures have been equalized.

and the focal length is $f = 150$ mm, we can obtain the spatial resolution (δd) of this STEAM system is around 44 μm

$$\delta d = f\delta\theta = \frac{fD}{\cos\theta}\delta\lambda. \tag{2}$$

To quantitatively characterize the imaging ability of the incoherent source based STEAM system, a resolution target (USAF 1951) was employed as the imaging sample, and its images are shown in Fig. 4. Before launching into the PASTA system, the spatially encoded spectral information was first detected by a conventional OSA, which realizes a standard spectrometer with accurate wavelength (0.05 nm) and good detection sensitivity (–60 dBm). The result is shown in the leftmost panel of Fig. 4, and the long time (0.2 s/frame) accumulated ASE source is quite stable. Replacing the OSA with the PASTA system to resolve the spectral information, the frame rate is greatly increased to 50 MHz (20 ns/frame), and the temporal aperture is ~5 ns. The ASE source within this short time span is essentially unstable, as shown in the second on the left of Fig. 4, which is greatly blurred due to the random fluctuated spectrum. Therefore, by increasing the averaging times of the PASTA frame, the reconstructed images are shown in Fig. 4 from the left to right. Obviously, the image quality is greatly improved with the increased progressively average times, and after averaged 50 times, the imaging quality is sufficiently stable. This 1-μs time span corresponds to 1-MHz frame rate—suitable for ultrafast imaging applications, such as web inspection and imaging flow cytometry.

It can be observed from Fig. 4 that our microscopic system can fully resolve the lines of the resolution target up to group 3, element 4, which corresponds to a resolution of 44 μm. This measured resolution matched well with the calculated results by Eq. (2), and it further verified that it is a diffraction-limited system. Based on Eq. (2), we decreased the focal length from 150 mm to 50 mm, to enhance the spatial resolution of the STEAM system by a factor of 3. Under this configuration, we selected a lens cleaning tissue as the sample under test, and the results are shown in Fig. 5. Similarly, it was still first observed using the OSA system, which is slow in terms of the frame rate, but can be treated

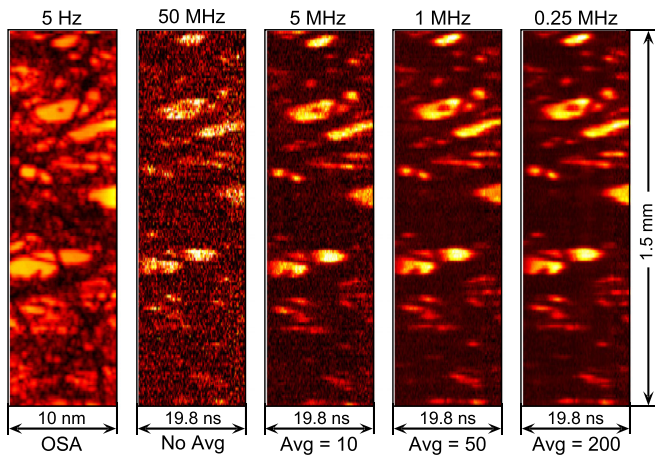

FIG. 5. Performance of imaging a lens cleaning tissue. From left to right, OSA: encoded wavelength information captured by the conventional OSA; No Avg: captured by the PASTA system, without averaging; Avg = 10–200: captured by the PASTA system, and each frame was averaged by 10 times, 50 times, and 200 times, respectively.

as an accurate and reliable reference. It can be observed from Fig. 5 that most of the features are well matched in all these images, though more detail structures can be observed using the OSA system, due to its better detection sensitivity (−60 dBm). The four images on the right of Fig. 5 are captured by the PASTA system with different averaging times, and it becomes stable after averaging by 50 times, consistent with the results as in Fig. 4.

In summary, we have leveraged the PASTA system to reconstruct the time-wavelength sequence from incoherent source, and demonstrated the time-stretch microscopy based on wideband incoherent source. In the conventional STEAM system, the direct temporal dispersion restricts the wideband source to be coherent ultrashort pulse. While the advance of the PASTA system greatly enlarged the temporal window by adding a focal time-lens in front of the temporal dispersion. Thus, it provides the possibility of reconstructing the time-wavelength sequence from arbitrary waveform, relaxing the requirement of the phase coherence of the light source. Therefore, by leveraging the PASTA system, the ASE based STEAM system has achieved the imaging bandwidth of 9-nm with 50-MHz frame rate. Although there is still a 0.5-nm pulse source in the PASTA system, this technology is still attractive by increasing the spectral efficiency by a factor of 18 (9 nm/0.5 nm). Owing to the unstable nature of the ASE source, it is preferable to accumulate 50 frames, to increase the spectral and temporal stability. Although the frame rate was scaled to 1 MHz, it is still sufficiently fast for most of the applications in high-throughput screening. Moreover, by converting the spatial information to the temporal domain, the optical signal is able to be amplified along the fiber medium, which benefits the time-stretch microscope in the imaging sensitivity. Besides the time-stretch microscopy, the concept of reconstructing the time-wavelength sequence is promising to find more applications, where wavelength is acted as the information carrier.

This work was partially supported by grant from the Research Grants Council of the Hong Kong Special Administrative Region, China (Project Nos. HKU 7172/12E, HKU 717510E, HKU 717911E, and HKU 720112E).

[1]K. Goda, K. K. Tsia, and B. Jalali, Nature **458**, 1145–1149 (2009).
[2]T. T. W. Wong, A. K. S. Lau, K. K. Y. Ho, M. Y. H. Tang, J. D. F. Robles, X. Wei, A. C. S. Chan, A. H. L. Tang, E. Y. Lam, K. K. Y. Wong, G. C. F. Chan, H. C. Shum, and K. K. Tsia, Sci. Rep. **4**, 3656 (2014).
[3]K. Goda, A. Ayazi, D. R. Gossett, J. Sadasivam, C. K. Lonappan, E. Sollier, A. M. Fard, S. C. Hur, J. Adam, C. Murray, C. Wang, N. Brackbill, D. D. Carlo, and B. Jalali, Proc. Natl Acad. Sci. U. S. A. **109**, 11630–11635 (2012).
[4]A. Mahjoubfar, C. Chen, K. R. Niazi, S. Rabizadeh, and B. Jalali, Biomed. Opt. Express **4**, 1618–1625 (2013).
[5]F. Xing, H. Chen, M. Chen, S. Yang, and S. Xie, Appl. Opt. **52**, 7049–7053 (2013).
[6]H. Chen, C. Wang, A. Yazaki, C. Kim, K. Goda, and B. Jalali, Appl. Opt. **52**, 4072–4076 (2013).
[7]K. K. Tsia, K. Goda, D. Capewell, and B. Jalali, Opt. Express **18**, 10016–10028 (2010).
[8]K. Goda, K. K. Tsia, and B. Jalali, Appl. Phys. Lett. **93**, 131109 (2008).
[9]A. Mahjoubfar, K. Goda, A. Ayazi, A. Fard, S. H. Kim, and B. Jalali, Appl. Phys. Lett. **98**, 101107 (2011).
[10]K. K. Tsia, K. Goda, D. Capewell, and B. Jalali, Opt. Lett. **34**, 2099–2101 (2009).
[11]K. K. Y. Cheung, C. Zhang, Y. Zhou, K. K. Y. Wong, and K. K. Tsia, Opt. Lett. **36**, 160–162 (2011).
[12]P. M. Moselund, M. H. Frosz, C. L. Thomsen, and O. Bang, Opt. Express **16**, 11954–11968 (2008).
[13]J. N. Kutz, C. Lyngå, and B. J. Eggleton, Opt. Express **13**, 3989–3998 (2005).
[14]D. R. Solli, C. Ropers, and B. Jalali, Phys. Rev. Lett. **101**, 233902 (2008).
[15]D. R. Solli, B. Jalali, and C. Ropers, Phys. Rev. Lett. **105**, 233902 (2010).
[16]G. Genty, J. M. Dudley, and B. Eggleton, Appl. Phys. B **94**, 187–194 (2009).
[17]C. Zhang, Y. Qiu, R. Zhu, K. K. Y. Wong, and K. K. Tsia, Opt. Express **19**, 15810–15816 (2011).
[18]C. Zhang, J. Xu, P. C. Chui, and K. K. Y. Wong, Sci. Rep. **3**, 02064 (2013).
[19]D. R. Solli, J. Chou, and B. Jalali, Nat. Photonics **2**, 48–51 (2008).
[20]C. Zhang, X. Wei, and K. K. Y. Wong, Opt. Express **21**, 32111–32122 (2013).
[21]C. Zhang, P. C. Chui, and K. K. Y. Wong, Appl. Opt. **52**, 8817–8826 (2013).
[22]C. Zhang, K. K. Y. Cheung, P. C. Chui, K. K. Tsia, and K. K. Y. Wong, IEEE Photonics Technol. Lett. **23**, 1022–1024 (2011).
[23]B. H. Kolner, IEEE J. Quantum Electron. **30**, 1951–1963 (1994).